Brain Research, 528 (1990) 238–244
Elsevier

BRES 15874

Correlations between unit firing and EEG in the rat olfactory system

Frank H. Eeckman and Walter J. Freeman

Department of Physiology–Anatomy, University of California at Berkeley, Berkeley, CA 94720 (U.S.A.)

(Accepted 20 March 1990)

Key words: Electroencephalographic origin; Electroencephalograph burst; Multi-unit recording; Olfaction; Cortical processing

The olfactory EEG of awake animals displays oscillatory bursts of activity in the γ- (30–100 Hz) range. The bursts are correlated with inflow of air over the receptor layer in the nose. None of the inputs to the cortices that display these oscillations carries periodic signals in the γ-range. Thus these bursts are generated locally, either by neuronal feedback interactions or by coupling of oscillatory neurons. In the first case if the oscillations are generated by negative feedback, then two classes of cells must exist: excitatory neurons and inhibitory neurons with the same frequency of oscillation but with a quarter cycle phase lag by the inhibitory cells from the excitatory cells. On the other hand, if the EEG's result from coupling of cells that are intrinsically oscillatory, there should be a broad but monomodal distribution of phase values. In order to determine the origin of these bursts, we performed simultaneous recordings of EEG and multi-unit spikes in the 4 parts of the olfactory system (olfactory bulb, anterior olfactory nucleus, prepyriform cortex and lateral entorhinal area) of awake and motivated rats. For each sample, the EEG and the multi-unit spikes were recorded from the same local neighborhood. The multi-unit electrode recorded pulses from the principal output neurons of the respective cortical areas. In all locations tested, the oscillations in pulse probabilities of firing were found to have the same frequency as the dominant EEG frequency. In all 4 structures two sets of cells were found. One set displayed pulses in phase with the EEG and the other set displayed pulses that led or lagged the EEG by approximately 1/4 cycle. These data confirm the negative feedback interaction model rather than the coupled oscillator model for the generation of the bursts in the olfactory system. The relevance of these findings to other cortical systems, in casu the visual cortex is discussed.

INTRODUCTION

The olfactory system of mammals generates nearly sinusoidal bursts of electrical activity (EEG) in the 30–100 Hz γ-range. These bursts ride on slow (1–7 Hz), high amplitude waves that are related to respiration. Each burst begins shortly after inspiration and terminates during expiration. None of the inputs to the olfactory bulb and cortex carries periodic signals in the γ-range. The high-frequency oscillations that are present in the olfactory system must therefore be generated locally. The goal of this study was to investigate further the relationship between neuron firing and cortical EEG by studying the statistical correlations between both EEG and pulse signals. In particular, we wanted to test some of the specific predictions of the negative feedback interactive model proposed by Freeman[7,8] for the generation of the burst, as compared with the coupled oscillator model of Llinas[15].

The architecture of the olfactory system is well known. Both the olfactory bulb and the olfactory cortex are simple 3-layered cortices (paleocortex). Each region has two main cell types: an excitatory projection cell and an inhibitory local interneuron. In the bulb, the mitral cells are the principal neurons and the granule cells are the local interneurons. In the cortex (including the anterior olfactory nucleus, the prepyriform cortex, and the lateral entorhinal area), the excitatory superficial pyramidal cells are the principal neuron and the inhibitory granule cells are the local interneurons. The principal cells in both structures are easily accessible to the investigator due to their large size and fixed position. Mitral cells, cortical pyramidal cells, and cortical granule cells fire large spikes that are easily detectable using extracellular electrodes.

The olfactory system offers a remarkable opportunity to test the negative feedback hypothesis for the following reason. In the bulb, the EEG is generated by the inhibitory interneurons (granule cells)[16,17], which do not have axons and do not generate extracellularly detectable action potentials. Hence the model predicts that the mitral cell units should oscillate with a 1/4 cycle phase lead over the EEG and there should be no class of cells that fires in phase with the EEG. In the cortex the EEG is generated by the excitatory superficial pyramidal cells. The pyramidal units should fire in phase with the EEG, whereas the interneuron units should fire with 1/4 cycle phase lag from the EEG. These relations are consistent

Correspondence: F.H. Eeckman. Present address: Lawrence Livermore National Laboratory, P.O. Box 808, Mailstop L-270, Livermore, CA 94550, U.S.A.

only with the negative feedback model and not with the coupled oscillator model.

MATERIALS AND METHODS

Adult male and female Sprague–Dawley rats (*Rattus norvegicus* sp.) were the experimental animal in this study. Linear stainless-steel electrode arrays, consisting of 6 elements spaced 250 μm apart were chronically implanted in the olfactory bulb and the olfactory cortex of all animals. A stimulating electrode pair was implanted in the lateral olfactory tract (LOT). The recording arrays were inserted so that a reversal of the LOT evoked potential occurred between the middle two electrodes. This placement of the array set the middle electrodes in the optimal position to record the activity of mitral cells in the bulb, and of pyramidal cells in the cortex[7]. In the cortex, the deeper electrodes were used to record granule cell activity.

All rats were allowed to recover for 3 days following surgery. They were then periodically motivated through mild food deprivation. Animals were kept at 90–95% of their presurgical weight. Water was provided ad libitum. During the recording session, the animal was maintained in its home cage inside a shielded chamber. The electrode connector set-up allowed virtually unrestricted movement. Recording sessions were typically 3 min long, and were taken while the animal was not moving inside the cage. No olfactory or electrical stimulation was used. Animals were always attentive and responsive to their environment, as judged by their response to unexpected sounds.

At the end of the recording sessions (1–2 weeks), the rats were sacrificed using a pentobarbital overdose. The rats were perfused with saline and formaldehyde, and their brains were explanted in formalin sucrose. Frozen sections were cut parasagittally at 50-μm intervals and stained with Cresyl violet. All electrode positions were verified microscopically.

Recording

Two channels of data were recorded concurrently for analysis. The EEG was filtered between 10 and 300 Hz. The unit signal was filtered between 300 and 3000 Hz and was sent through a window discriminator, adjusted to emit a standard 5 V, 1.2 ms wide pulse every time the signal fell into a preset window. The minimum threshold level was set at 2–3 times the background noise level. The unit signal typically contained multiple (3–4) different spike waveforms and all of these were represented by identical standard pulses. Both EEG and pulses were recorded on-line, multiplexed (channel offset 10 μs) and digitized at 1 ms time intervals. They were stored on disk on a Perkin-Elmer 3220 for off-line analysis.

Analysis

Data analysis techniques have been discussed previously[4,7]. Briefly, the following steps were taken.

Editing. Both EEG and pulses were displayed simultaneously on a digital scope, and all sections corresponding to EEG burst segments (100–200 ms) were visually edited into a separate data file. All data files consisted of 2-channel data. The average number of segments per file was 53.

Processing. EEG amplitude histograms were calculated for all the EEG values within a record. These histograms resemble a Gaussian probability density function. They are described by their mean, standard deviation, skewness, and kurtosis coefficients. Normality tests were performed on the data in the histogram.

A lag-time histogram and an expectation density function were computed for the pulses in each file. These graphs were used to distinguish between single-unit and multi-unit traces[7].

The Two Dimensional Conditioned Pulse Probability Table was used to find correlations between units and EEG[4,7]. This table gives the probability of occurrence of a spike conditional on time and on normalized EEG amplitude value. The table is constructed in the following way. For every occurrence of an EEG value (ΔV) in the stored time series one checks whether a pulse was recorded at the same time ($T = 0$) or in any of the preceding 25 ($T = -25$) or following 25 ($T = +25$) timebins. If a pulse was recorded a value of 1 is added to the table at a location corresponding to the relative time (–25 to +25 ms) and EEG value (-3σ to $+3\sigma$) at which that pulse occurred. The number of pulses n_p for each time and amplitude interval is then divided by the total number of pulse-amplitude pairs. The resulting pulse density in time and amplitude is divided by the amplitude probability density. This yields the pulse probability conditional on time and amplitude.

An average pulse probability vs time was formed by summing the distributions in the two-dimensional table from $+1\sigma$ to $+3\sigma$ and dividing these by the number of bins. Similarly for -1σ to -3σ. These two functions are usually oscillatory functions of pulse probability on time. They are approximately mirror images of one another. The difference of the two functions divided by two is called the experimental pulse probability wave (PPW). It is fitted by one of the following equations:

$$P(T) = p_0\{1 + \tilde{p}\cos(\omega T + \phi)\exp^{-\alpha|T|}\} \quad (1)$$

$$P(T) = p_0\{1 + \tilde{p}\,[\cos(\omega_1 T + \phi_1)\exp^{-\alpha_1|T|} + \cos(\omega_2 T + \phi_2)\exp^{-\alpha_2|T|}]\} \quad (2)$$

where p_0 is the steady state pulse rate, and $\tilde{p}$ is the modulation amplitude.

The following parameters will be used to describe the PPW. The frequencies ω_i in radians ($\omega_i = 2\pi f_i$; f_i in Hz), the phases ϕ_i in radians, and α_i the decay coefficients. The PPW is analogous to a cross correlogram.

Power spectra

Estimation of power spectra was done using the fast fourier transform (FFT) algorithm for the following data sets. (1) the EEG segments contained in the data files; (2) the PPW, a cross section through the conditional probability table; and (3) the residuals of the PPW after fitting a first sine wave.

Curve fitting

The algorithm for estimating model parameters is a non-linear regression based on the Levenberg–Marquardt algorithm[11]. It requires initial guesses for the non-linear parameters only. These guesses were obtained from the FFT. The total spectral energy incorporated in the fit is used to determine the goodness-of-fit. PPWs and their residuals were fitted using this algorithm.

RESULTS

Qualitative description of the EEG

In awake and motivated rats 5–25-s periods of bursting EEG alternate with 15–45-s periods of non-bursting, resting EEG. This cycling is matched to the behavior of the animal. The bursting stages correspond to exploratory behavior, while the resting stages correspond to relative indifference to the environment. This periodicity is present in all awake animals, whether food deprived or not. It is independent of the presence or absence of applied odors. During odor application, however, the frequency and the duration of the bursting periods increases. This increase is even more dramatic in food deprived animals.

The fundamental characteristics of the olfactory EEG are high frequency bursting and the presence of a respiratory wave. These characteristics are modified in the following way as one moves the electrode from the

periphery (OB) to more central locations (posterior PPC and lateral entorhinal areas (LEA)): (1) the amplitude of the slow wave decreases, and in some posterior positions the wave is absent altogether; (2) the bursts decrease in frequency, but especially in amplitude and duration, while the amplitude of the interburst segment increases. Therefore, bursts are less conspicuous in the posterior cortex; (3) in the medial and posterior entorhinal areas, rhythmic slow activity (RSA) becomes visible during motivation. RSA or θ activity (4–6 Hz) has been well documented, and unit activity related to its frequency has been described by Alonso and Garcia-Austt[1].

Data used

This paper is based on data contained in 223 files, taken from 54 subjects. They represent 11,872 bursts, i.e. an average of 53 bursts per file. Each file contains all the bursts and their associated spikes that were present in one session recorded from one site.

Power spectra

The power spectra of bursts from the olfactory bulb (4235) have a single peak in the 60–90 Hz range. Most peaks occur at around 75 Hz. The distribution of amplitude values is Gaussian, with a mean coefficient of kurtosis (mck) of 3.2 ± 0.6. The power spectra of bursts recorded from the anterior olfactory nucleus (AON) (1008 bursts) are similar to those of the olfactory bulb in all respects.

In the PPC, however, 17% of the bursts (846 out of 4976) show more than one peak in their power spectrum. Of these 17%, a third show a second peak greater than 1/2 of the dominant peak.

In the LEA, 60% of the bursts (992 out of 1653) have a single peak, while 40% have two peaks. In 50% of the latter group, the second peak is greater than 1/2 of the amplitude of the dominant peak.

Amplitude histogram

The distribution of EEG amplitude values in each record is nearly Gaussian in shape. In all cases the mean amplitude was close to 0 mV. All distributions (223) are normal as evidenced by the standard normality test. The mean mck for all records is 3.2 ± 0.6.

Pulses

The average number of pulses for the entire data set is 30 pps. Considering an average firing rate for cortical cells of 5–10 pps, this would indicate that 3–6 units were present in most records.

Unit-EEG correlations

For all 223 files, a pulse-probability wave (PPW) was calculated using the method described above. These PPWs were fitted with Eqn. 1. The frequency of fit (FOF), the phase (ϕ), and the decay constant (α) are used to describe the PPW. The peak frequency of the bursts in the EEG (FOB) was calculated for comparison.

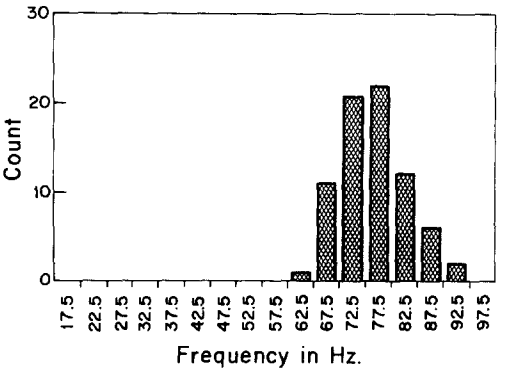

Fig. 1. Correlation between multi-unit spikes and EEG in the olfactory bulb. The graph shows the distribution of frequencies obtained through fitting equation 1 to the pulse probability waves (PPW). There are 75 cases, recorded in 24 subjects. The mean value is 77.0 ± 6.3 Hz. The distribution is nearly Gaussian in shape.

Olfactory bulb

There are 75 data files, recorded in 24 subjects.

Frequency. Units were correlated with the EEG at a mean frequency (FOF) of 77.0 ± 6.3 Hz. The median is 77.0 Hz. The extreme values range from 62.0 to 95.0 Hz. The distribution of correlated frequencies is nearly Gaussian, except for being slightly skewed to the right as shown in Fig. 1.

The dominant frequency of EEG bursts (FOB) is 74.5 ± 5.7 Hz. The median is 73.8 Hz and the range extends from 64.0 to 93.5 Hz. The PPW and the dominant frequency of the EEG are strongly correlated. The correlation coefficient is 0.85.

Phase. The mean phase is +1.6 ± 0.6 radians. The distribution has a range of 2.5 radians.

Decay coefficient. The average value is 0.043 ± 0.023, with a median value of 0.043.

Anterior olfactory nucleus

There are 18 files, recorded from 7 subjects.

Frequency. The mean FOF is 76.1 Hz with a standard deviation of 4.2 Hz. The median FOF is 76.5 Hz. The extreme values range from 69.0 to 83.0 Hz. The dominant frequency of bursting in the EEG has a mean value of 74.3 ± 3.5 Hz. The median value is 74.3 Hz and the range extends from 68.6 to 82.3 Hz. The correlation coefficient relating the FOF to the dominant frequency of the EEG bursts is 0.80.

Phase. There are two types of cells that fire spikes in the AON. Pyramidal cells in layer 2 and granule cells in

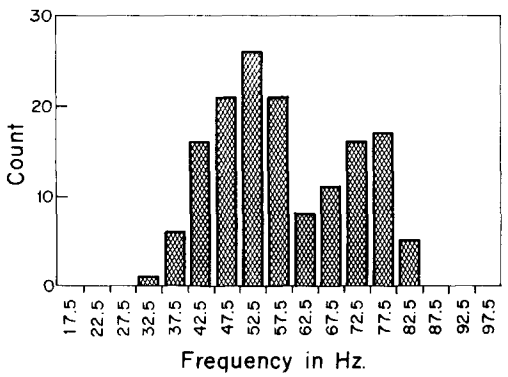

Fig. 2. Distribution of correlated frequencies for data obtained from the olfactory cortex. Data from the anterior nucleus (AON), the prepyriform cortex (PPC), and the lateral entorhinal areas (LEA) are pooled together in this graph. There are 148 cases. The distribution is bimodal in shape. The high-frequency lobe peaks at 77.5 Hz and overlaps with the distribution of correlated frequencies recorded from the olfactory bulb (see Fig. 1).

layer 3. The pyramidal cells are the generators of the EEG signal. Their mean phase was 0.4 ± 0.3 radians. The median was 0.4 radians. For the granule cells the mean value was −1.5 ± 0.2 radians, with a median of −1.6 radians.

Decay coefficient. The average value is 0.058 ± 0.026, with a median value of 0.056.

Prepyriform cortex

There are 98 records, recorded from 30 subjects.

Frequency. The mean frequency of the PPWs is 54.3 ± 11.5 Hz. The median is 53.0 Hz. The range extends from 34.0 to 82.0 Hz. The distribution of values is bimodal with a low mode of 53.0 ± 5.6 Hz and a high mode of 73.0 ± 6.2 Hz. The dominant frequency of EEG bursting has an average value of 54.3 ± 10.5 Hz. The median frequency is 53.3 Hz. The distribution is also bimodal. The high mode occurs at 75 ± 5.8 Hz, while the low mode is positioned at 54 ± 6.4 Hz. The correlation coefficient relating PPW to the dominant frequency in the EEG is 0.95.

Phases. There are two types of cells that fire spikes in the PPC. Pyramidal cells in layer 2 and granule cells in layer 3. Freeman has labeled these class A and class B cells, respectively[6]. The pyramidal cells are the generators of the EEG signal. Their mean phase is 0.1 ± 0.4 radians. The median value is 0.1 radians. For the granule cell the mean value of −1.8 ± 0.4 radians. The median value in this group is −1.7 radians. Class A and class B cells are identically distributed over the two frequency modes.

Decay coefficient. The average value is 0.053 ± 0.031, with a median value of 0.052.

For 15 records, two frequencies could be fitted to the

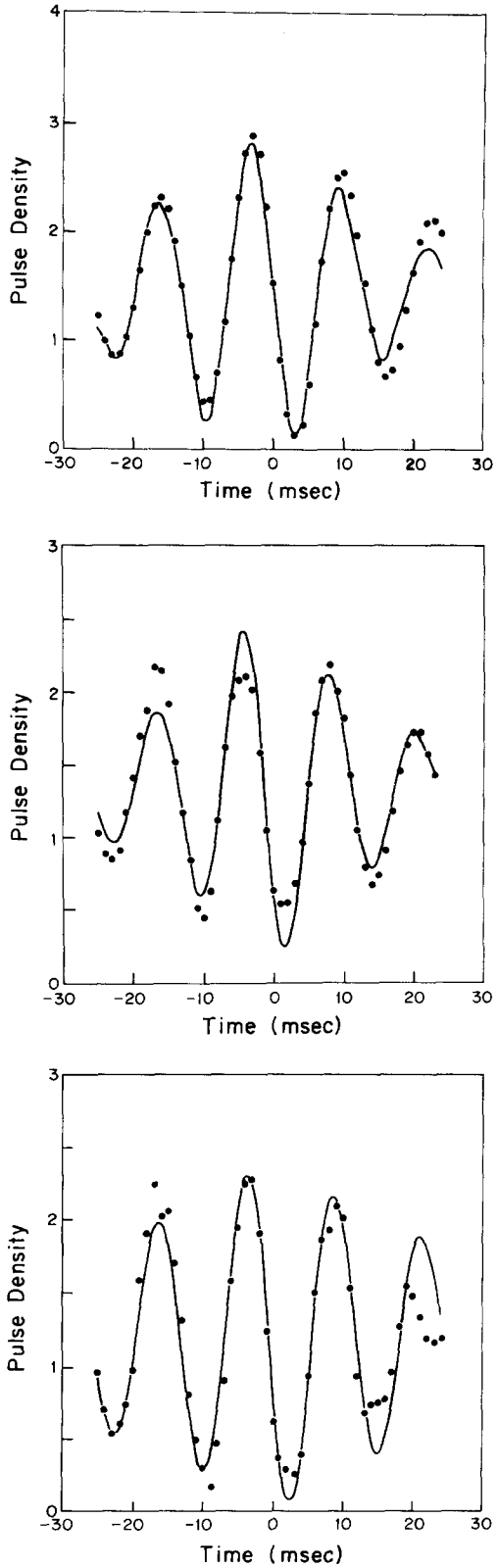

Fig. 3. Some examples of pulse probability waves obtained from the olfactory bulb. The dots represent the data points. The solid lines are the results of fitting Eqn. 1 to the data. Note that the pulse maximum leads the EEG by approximately a quarter cycle. The graphs are cross sections through the 2D table (see Methods). They are analogous to cross-correlograms. Time on the *X*-axis is measured relative to the EEG maxima. Pulse density is a dimensionless quantity related to firing probability.

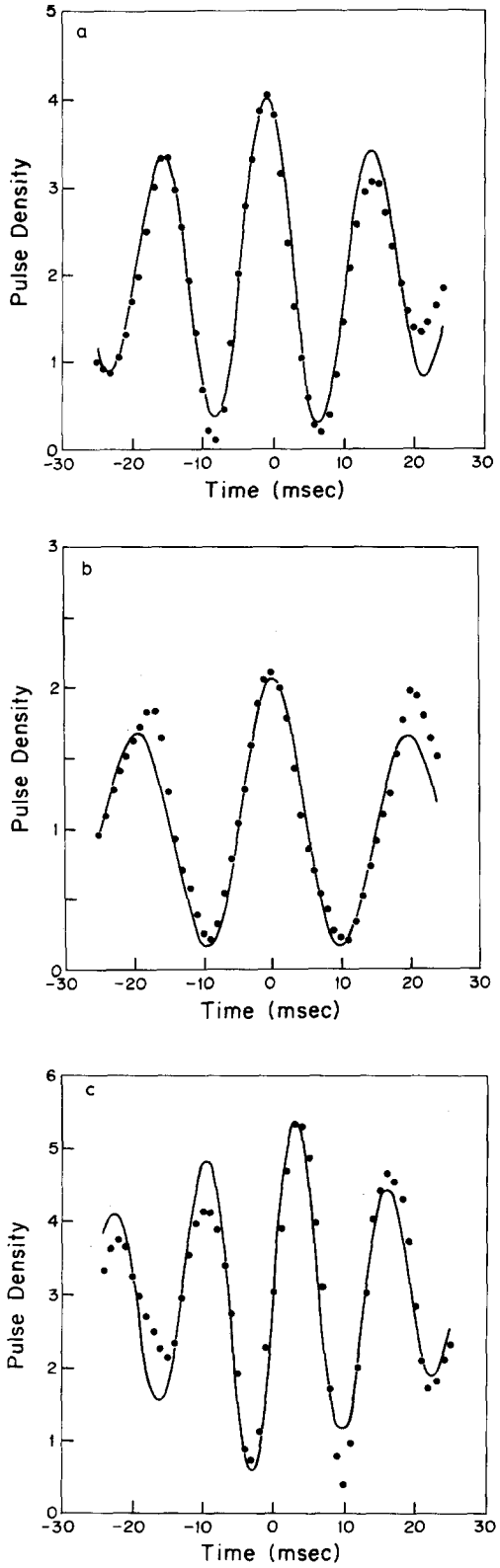

Fig. 4. Some examples of PPWs obtained from the prepyriform cortex. The dots represent the data points. The solid lines are the result of fitting Eqn. 1 to the data. In the cortex, two sets of cells are present: Type A cells, whose maximal firing probability is in phase with the EEG (a,b) and Type B cells, whose firing lags the EEG maximum by a quarter cycle (c). Time on the X-axis is measured relative to the EEG maxima. Pulse density is a dimensionless quantity related to firing probability.

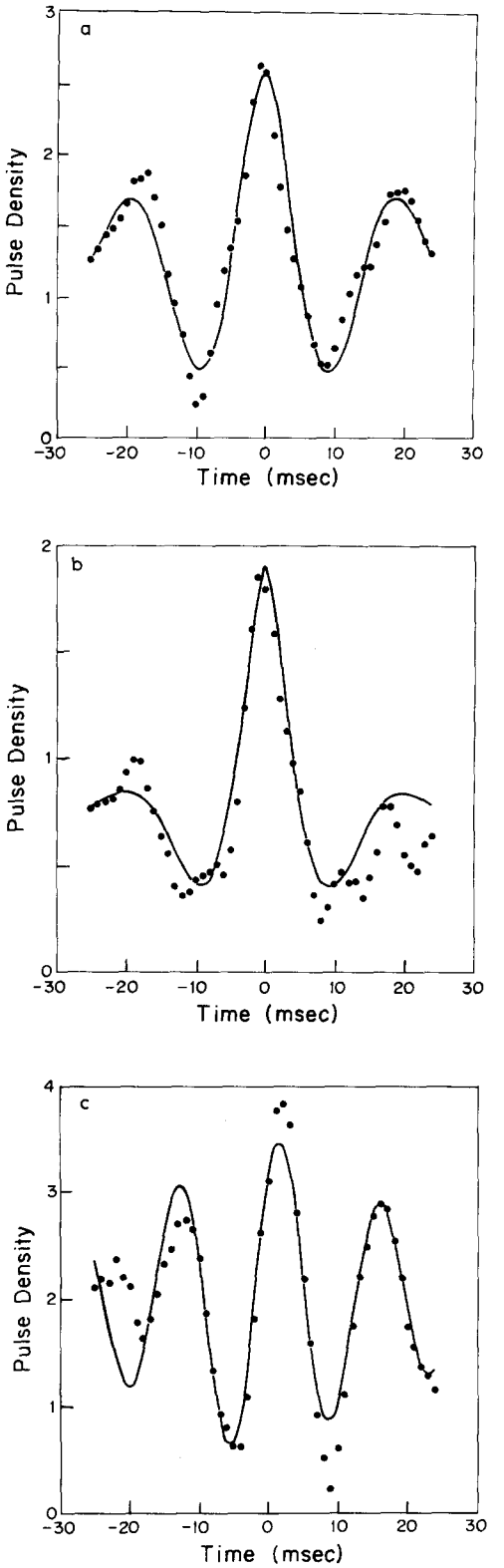

Fig. 5. Some examples of PPWs obtained from the lateral entorhinal area. The dots represent the data points. The solid lines are the result of fitting Eqn. 1 to the data. In the lateral entorhinal area, two sets of cells are present: Type A cells, whose maximal firing probability is in phase with the EEG (a,b) and Type B cells, whose firing maximum lags the EEG maximum by a quarter cycle (c). Time on the X-axis is measured relative to the EEG maxima. Pulse density is a dimensionless quantity related to firing probability.

TABLE I

Summary of results

This table summarizes the results obtained in the different olfactory areas. It compares the frequencies obtained through fitting Eqn. 1 to the PPW with the dominant frequency of the bursts in the olfactory EEG. The dominant frequency of oscillation of the EEG is strongly correlated to the PPW in all cases (correlation coefficients >0.9 in all areas).

Dominant frequency of bursts	*Unit/EEG cross-correlation*
Olfactory bulb (75 data-files)	
Gaussian distribution	Gaussian distribution of frequencies
74.5 ± 5.7 Hz	77.0 ± 6.3 Hz
	Phase at time 0 = 1.6 ± 0.6 radians
Anterior olfactory nucleus (18 data-files)	
Gaussian distribution	Gaussian distribution of frequencies
74.3 ± 3.5 Hz	76.1 ± 4.2 Hz
	Phase at time 0 =
	+0.4 ± 0.3 radians (class A)
	−1.5 ± 0.2 radians (class B)
Prepyriform cortex (98 data-files)	
Bimodal distribution	Bimodal distribution of frequencies
54.3 ± 10.5 Hz	54.3 ± 11.5 Hz
Modes	Modes
54.0 ± 6.4 Hz	53.0 ± 5.6 Hz
75.0 ± 5.8 Hz	73.0 ± 6.2 Hz
	Phase at time 0 =
	+0.1 ± 0.4 radians (class A)
	−1.8 ± 0.4 radians (class B)
Lateral entorhinal area (32 data-files)	
Bimodal distribution	Bimodal distribution of frequencies
56.3 ± 9.7 Hz	58.8 ± 10.3 Hz
Modes	Modes
52.0 ± 6.4 Hz	52.5 ± 6.5 Hz
70.0 ± 5.1 Hz	70.0 ± 5.2 Hz
	Phase at time 0 =
	+0.1 ± 0.2 radians (class A)
	−1.6 ± 0.3 radians (class B)

PPW. This was done using Eqn. 2. Nine belonged to class A (units in phase with EEG), while 6 belonged to class B (units lagging the EEG). The mean value for the high frequency is 68.5 ± 8.7 Hz. The median is 69.3 Hz. The mean value for the lower frequency is 39.1 ± 7.1 Hz. The median is 35.2 Hz. These two frequencies are not harmonically related to one another. The phase distributions and decay coefficients are no different than the ones for single frequency fits. The mean phase differences between the phases associated with the high frequency and the phases associated with the low frequency are 0.3 radians for both groups.

Lateral entorhinal area

Frequency. The mean FOF is 58.8 Hz. The standard deviation is 10.3 Hz. The extreme values were 40.0 and 77.0 Hz. The distribution is bimodal with peaks at 52.5 ± 6.5 Hz and 70.0 ± 5.2 Hz. The dominant frequency for bursts in the EEG is 56.3 ± 9.7 Hz. The median value is 56.5 Hz. The extremes are 39.2 and 78.4 Hz. The frequency values of the PPW are strongly correlated to the dominant frequency of the bursts. The correlation coefficient was 0.95.

Phase. Two kinds of traces are present. For the class A pyramidal cells (18 observations) the mean phase value is 0.1 ± 0.2 radians. The median is 0.1 radians. For the class B granule cells (14 observations) the mean phase is −1.6 ± 0.3. The median is −1.6.

Decay. The mean decay value is 0.071 ± 0.048. The median value is 0.060.

The data from the cortical areas (AON, PPC, and LEA) were pooled into one group. The distribution of the pooled FOFs for the cortical regions is shown in Fig. 2. Figs. 3–5 show some examples of PPWs fitted with sine functions. Table I summarizes the results of this study.

Failure rate

We searched for unit-EEG correlations using all electrode pairs with adequate position as shown by a reversal of the evoked potential and by subsequent histology. In about 25% of the cases it was impossible to fit the PPW with either equation 1 or 2 within the accepted goodness of fit criteria (>85% of variance explained by fitting the curve). These records were classified as failures. Failures include not only records with neuron firing that is unrelated to the EEG signal but also cases of electrode malfunction and damage to the tissues.

Interburst period

We tested all interburst segments in continuous 5-min recordings in 5 subjects. No correlations between EEG and spikes were present in these segments. In the same subjects we also tested both continuous and burst records and found no difference in the calculated PPWs between the two. Both showed strong correlations with frequencies within ± 0.5 Hz and phases within ± 0.2 radians. This justifies the selection of burst segments for analysis.

DISCUSSION

In this study we have investigated the relationship between neuron firing and cortical EEG patterns in the olfactory system of awake rats. We found that unit firing probability is strongly correlated to EEG maxima in the awake animal. This correlation occurs at different phase values depending on the location of the electrodes in the olfactory system. The phase values found in this study correspond to those predicted by the negative feedback model[7,8]. As predicted, in the olfactory bulb, the maximum unit firing probability leads the EEG maximum by a quarter cycle. In the olfactory cortex, two types of cells

were found: one population fires in synchrony with the EEG, while the other population lags the EEG maximum by a quarter cycle.

The maximum phase error in our calculations was estimated as follows. The systematic error due to digitizing and multiplexing is no greater than 0.4 radians phase lag for the pulses to EEG for a 80-Hz signal. The error due to electrode position with respect to the cell layer that generates the signal has a maximal value of ± 0.7 radians[6]. This error is due to the curvature of the cortex and the spread of the signal across the surface. In our study the sign of this error is random and time varying. It would therefore tend to cancel out.

In theory it is possible for a bimodal distribution of phase values to exist between one population of oscillatory cells that is coupled together, and a second such population that is driven by the first over an axonal pathway that provides a propagation delay. In this case the phase lag of the driven population from that of the driving population must increase with the driving frequency. An example is shown by Bressler[2] in the phase relations between the bulb and the prepyriform cortex. However in our study no correlation was found between phase and frequency for records from within the bulb and cortex, which provides additional evidence against the coupled oscillator hypothesis of Llinas[15] and others.

Negative feedback between two populations of interacting neurons as a basis for oscillation is a key feature in the Freeman model[6–9]. It is compatible with the recent current source density findings in the opossum prepyriform cortex by Rodriguez and Haberly[18]. Negative feedback is also present in the Li and Hopfield model for olfactory bulb processing[13,14]. In their model for the PPC, Wilson and Bower[19] do not attribute the origin of the oscillation to the local negative feedback. They stress the importance of long range feedback interactions between different parts (anterior and posterior) of the cortex. The data presented here do not allow us to assess the importance of long-range interactions in the generation of oscillatory bursts. The data do show, however, that short-range negative feedback interactions between superficial pyramidal cells and cortical granule cells are a sufficient mechanism for bursting.

The importance of negative feedback as a basis for oscillation is further underlined by the discovery of information-bearing γ-oscillations in the primary visual cortex of the monkey[10], and the existence of correlations between high frequency oscillatory EEG and unit firing in various visual areas by Gray et al.[12] and by Eckhorn et al.[3]. Correlations between the inhibitory neurons and cortical EEG should be studied in these areas as well.

Acknowledgement. This study was supported by Grant MH06686 from the National Institute of Mental Health.

REFERENCES

1 Alonso, A. and Garcia-Austt., Neuronal sources of theta rhythm in the entorhinal cortex of the rat. II. Phase relations between unit discharges and theta field potentials, *Exp. Brain Res.*, 67 (1987) 502–509.
2 Bressler, S.L., Relation of olfactory bulb and cortex. II. Model for driving of cortex by bulb, *Brain Research*, 409 (1987) 294–301.
3 Eeckhorn, R., Bauer, R., Jordan, W., Brosch, M., Kruse, W., Munk, M. and Reitboeck, H.J., Coherent oscillations: a mechanism of feature linking in the visual cortex? *Biol. Cybernetics*, 60 (1988) 121–130.
4 Eckman, F.H. and Freeman, W.J., The sigmoid nonlinearity in neural computation: an exprimental approach. In J.S. Denker (Ed.), *Neural Networks For Computing, AIP Conference Proceedings, Vol. 151*, 1986, pp. 135–139.
5 Freeman, W.J., Distribution in time and space of prepyriform electrical activity, *J. Neurophysiol.*, 22 (1959) 644–665.
6 Freeman, W.J., Relation between unit activity and evoked potentials in prepyriform cortex of cats, *J. Neurophysiol.*, 31 (1968) 337–348.
7 Freeman, W.J., *Mass Action in the Nervous System*, Academic, New York, 1975.
8 Freeman, W.J., Nonlinear gain mediating cortical stimulus response relations, *Biol. Cybernetics*, 33 (1979) 237–247.
9 Freeman, W.J., Simulation of chaotic EEG patterns with a dynamical model of the olfactory system, *Biol. Cybernetics*, 56 (1987) 139–150.
10 Freeman, W.J. and van Dijk, B.W., Spatial patterns of visual cortical fast EEG during conditioned reflex in a rhesus monkey, *Brain Research*, 422 (1987) 267–276.
11 Golub, G.H. and Peyera, V., The differentiation of pseudo-inverses and nonlinear least squares problems whose variables separate, *Soc. Ind. Appl. Math. J. Num. Anal.*, 10 (1973) 413–432.
12 Gray, C.M., Koenig, P., Engel, A.K. and Singer, W., Oscillatory responses in cat visual cortex exhibited inter-columnar synchronization which reflects global stimulus properties, *Nature*, 338 (1989) 334–337.
13 Li, Z., A model of olfactory adaptation and sensitivity enhancement in the olfactory bulb, *Biol. Cybernetics*, in press.
14 Li, Z. and Hopfield, J.J., Modeling the olfactory bulb and its neural oscillatory processings, *Biol. Cybernetics*, 61 (1989) 379–392.
15 Llinas, R.R., Electrophysiological properties of mammalian neurons: insights into central nervous system function, *Science*, 242 (1988) 1654–1663.
16 Mori, K. and Takagi, S.F., An intracellular study of dendrodendritic inhibitory synapses on mitral cells in the rabbit olfactory bulb, *J. Physiol.*, 279 (1978) 569–588.
17 Rall, W. and Shepherd, G.M., Theoretical reconstruction of field potentials and dendrodendritic synaptic interactions in the olfactory bulb, *J. Neurophysiol.*, 31 (1968) 884–915.
18 Rodriguez, R. and Haberly, L.B., Analysis of synaptic events in the opossum pyriform cortex with improved current source-density techniques, *J. Neurophysiol.*, 61 (1989) 702–718.
19 Wilson, M. and Bower, J., A computer simulation of olfactory cortex with functional implications for storage and retrieval of olfactory information. In D.Z. Anderson (Ed.), *Neural Information Processing Systems*, Am. Inst. Physics, New York, 1988, pp. 114–126.